Observation of an optical Wannier-Stark ladder

C. Martijn de Sterke,[1] J. N. Bright,[1] Peter A. Krug,[2] and T. E. Hammon[3,4]
[1]*School of Physics, University of Sydney, Sydney 2006, New South Wales, Australia*
[2]*Australian Photonics Cooperative Research Centre, Australian Technology Park, Eveleigh 1430, Australia*
[3]*Indx Propriety Ltd., Australian Technology Park, Eveleigh 1430, Australia*
[4]*Department of Electrical Engineering, University of Sydney 2006, Australia*
(Received 24 September 1997)

We report the observation of an optical Wannier-Stark ladder in a linearly chirped Moiré grating, written in the core of an optical fiber. The use of photons avoids the strong excitonic interactions encountered in more traditional experiments using charge carriers in semiconductors. [S1063-651X(98)06402-2]

PACS number(s): 42.25.Bs, 42.81.Dp, 78.20.Jq

I. INTRODUCTION

The Wannier-Stark ladder (WSL) is a concept with a distinguished pedigree. Briefly, in 1959 it was proposed theoretically by Wannier to exist in crystalline solids subject to a uniform electric field [1]. The essential elements of the WSL are illustrated in Fig. 1. Consider first Fig. 1(a), which shows schematically three trajectories of a charged particle (solid lines) in a uniform electric field. The field is indicated by the linearly varying potential, using the dashed line. A particle initially traveling to the right is decelerated by the field and is reflected at a position that depends on its initial energy. Figure 1(b) shows how charged particles in a periodic potential in addition to the uniform field can undergo *Bloch oscillations*: Consider a particle that is just being reflected by the uniform component of the field. Since it is momentarily at rest, its associated de Broglie wavelength, which is inversely proportional to its momentum, diverges. Upon being accelerated to the left in Fig. 1(b), its momentum increases and thus the de Broglie wavelength shrinks. Eventually the de Broglie wavelength reaches the Bragg wavelength associated with the periodic component of the potential. The particle is then Bragg reflected and travels to the right. Traveling to the right, it is decelerated by the field, until it is reflected by the linear component of the potential. The process then repeats itself. Thus, in a periodic potential with a uniform electric field the particles' trajectories are closed: They are localized in periodic orbits, in which they are reflected by the uniform field on one side [as in Fig. 1(a)] and by Bragg reflection on the other. Translational symmetry implies that there would be a (Wannier-Stark) ladder of such states, exhibiting the WSL's defining characteristics: Adjacent states are displaced by a lattice constant and the spacing in energy between adjacent states equals the potential drop per period [1]. We note that in Fig. 1(b) the Bragg reflection can be considered to originate from a sideband of the potential, spawned by the potential's periodic component.

Since Wannier's original work, research has developed along two different lines. The first has concentrated on the nature of the WSL rungs. It has raised considerable controversy [2–4], which only recently seems to have been resolved with the conclusion that, strictly speaking, the rungs are resonances with finite lifetime, but not exact eigenstates [4,5]. The second line of research has concentrated on the experimental observation of WSLs. The first unambiguous observation, in a semiconductor superlattice [6], demonstrated that the description given above is incomplete: The electron-hole interaction in semiconductors dominates the external field, so that, in effect, an excitonic WSL is observed [6,7]. Though these are well understood and the electron-hole interaction is unimportant in certain limits [7], excitonic WSLs lack the compelling simplicity of Wannier's original proposal. Clearly, its observation requires neutral species, such as atoms or photons. Observations of atomic WSLs have been reported recently [8–10]. Here, following earlier theoretical work [11,12], we report the observation of an *optical* WSL (line 1 of Table I).

In previous proposals for optical WSLs it was argued that the optical equivalent of the uniform electric field in the electronic problem is a linearly varying refractive index [11,12] and that the reflection of electrons by such a field is analogous to total internal reflection [11]. However, since the latter cannot be achieved at normal incidence with dielectrics only, it was proposed to use non-normal incidence [11], hence adding considerable complexity to the geometry. For this reason this proposed geometry was never realized.

Here we propose and demonstrate that a WSL can be

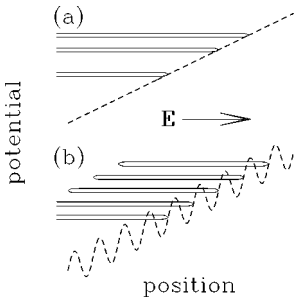

FIG. 1. (a) Possible trajectories of charged particles in a uniform electric field; the field direction indicated applies to negatively charged particles. Moving initially to the right, the particles are decelerated by the field and reflected at a position that depends on the initial energy. Shown in (b) is the corresponding result when the potential also has a periodic component. Particles can then undergo Bloch oscillations, in which they are localized by the electric field on the right-hand side and by Bragg reflection on the left.

TABLE I. Comparison of corresponding concepts from the electronic and the optical WSL.

Electronic WSL	Optical WSL
electron	photon
uniform field (linear potential)	linear chirp
lattice constant	Moiré period
periodic crystal potential	periodic κ
potential drop per period	chirp per period

observed in a chirped Moiré grating, which is written in the core of an optical fiber. Even though such gratings have been fabricated before [13], the key point of interest here is the interpretation of the transmission spectrum of such gratings. This spectrum consists of approximately equally spaced transmission fringes [13], which we interpret as rungs of an optical WSL.

This paper is structured as follows. In Sec. II we explain why chirped Moiré gratings allow one to observe an optical WSL. In Sec. III we describe the fabrication of such a grating and analyze its spectrum in terms of an optical WSL. We briefly discuss our results and conclude in Sec. IV.

II. BACKGROUND

As mentioned, here we propose and demonstrate an optical WSL in a one-dimensional, chirped Moiré grating [13], written in the core of an optical fiber. To understand why this leads to an optical WSL we briefly review some key properties of gratings. We consider gratings in which the light travels perpendicularly to the rulings; then in a *uniform* grating the light is Bragg reflected in a spectral region centered about the Bragg frequency f_B. For first-order Bragg reflection [14,15]

$$f_B = \frac{c}{2\bar{n}d}, \tag{2.1}$$

where $\bar{n}$ is the average refractive index and d is the grating period. The range over which Bragg reflection occurs corresponds to the photonic band gap of the grating [16]; it is well known [14,15] that its width Δf_{bg} is given by

$$\Delta f_{\mathrm{bg}} = \frac{\Delta n}{\bar{n}} f_B \equiv \frac{c}{\pi \bar{n}} \kappa \tag{2.2}$$

defining the coupling coefficient κ, which represents the grating strength per unit length. The parameter Δn is the depth of the grating's refractive index modulation, corrected for the imperfect overlap between the grating and the optical field.

We next consider a *linearly chirped* grating, a grating in which $1/d$ is a linear function of position. The properties of chirped gratings are well known: Since $1/d$ varies linearly with position, so does f_B [Eq. (2.1)]. Thus different frequencies (energies) are reflected at different positions along the grating [14,17]. This is illustrated in Fig. 2(a), which shows the two edges of the photonic band gap as a function of position for a linearly chirped grating (short- and long-dashed lines). At a given position, frequencies between these two lines correspond to the photonic band gap. Thus, for these frequencies the grating acts as a mirror, while for other frequencies the grating is essentially transparent [14]. The linear dependence of position of these two lines indicates the linear chirp [see Eq. (2.1)]; the constant separation indicates that the width of the photonic band gap is constant. In turn, by Eq. (2.2), this indicates that Δn, and thus κ, is constant. Shown in Fig. 2(a) by the solid lines are a few typical light trajectories: Different frequencies are all reflected, but at positions that depend linearly on frequency (this statement assumes that the grating is sufficiently strong; this is certainly true for the grating described in Sec. III). Of course this property is identical to the key characteristic of the reflection of a charged particle by a uniform electric field as schematically indicated in Fig. 1(a) (see also line 2 of Table I). In contrast to previously proposed optical geometries [11,12], therefore, in a chirped grating there is no need for nonnormal incidence to mimic the electric field and the one-dimensional character of the WSL can thus be preserved.

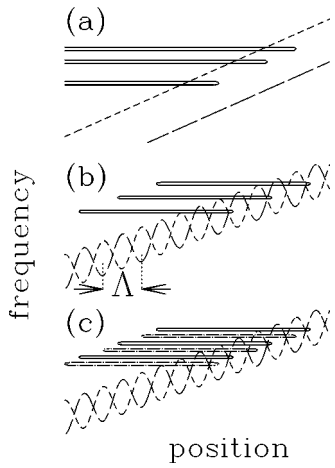

FIG. 2. Photonic band diagrams for two types of gratings showing the two edges of the photonic band gap as a function of position (short- and long-dashed lines). That in (a) is for a linearly chirped grating, (b) and (c) are for a chirped Moiré grating. Also shown are some typical light trajectories using solid and dash-dotted lines. Note the similarity to Fig. 1.

Now that we have ''used'' a chirped grating to achieve the effect of a uniform electric field, we cannot employ its periodicity again to obtain the optical analog of the Bragg reflection of electrons. We must thus obtain the effect of the periodicity from elsewhere. To do so, we use a grating that has a periodicity in addition to the basic period d of the refractive index. Such superstructure gratings [18,19], or optical superlattices [20], were studied earlier in various experimental geometries [18,19] and can be obtained by letting at least one of the parameters d, $\bar{n}$, or Δn vary periodically with position. The particular type of superstructure grating we use is a Moiré grating [13], in analogy to the well-known Moiré effect. Moiré gratings can be fabricated by superimposing two gratings with slightly different periods d_1 and d_2, but otherwise identical, in the same length of fiber. It is easy to see that, due to the beating of the two underlying gratings, Moiré gratings have a large Moiré period Λ, given by

$$\frac{1}{\Lambda}=\frac{1}{2}\left|\frac{1}{d_1}-\frac{1}{d_2}\right|; \tag{2.3}$$

it is this large Moiré period that is analogous to the crystal period in the electronic WSL (line 3 of Table I).

A more quantitative understanding of our geometry is obtained by considering the Moiré grating's refractive index distribution

$$n(z)=\overline{n}+\delta n\,\cos\left(\frac{2\pi z}{d_1}\right)+\delta n\,\cos\left(\frac{2\pi z}{d_2}\right)$$

$$\equiv\overline{n}+\Delta n(z)\cos\left(\frac{2\pi z}{D}\right), \tag{2.4}$$

where Δn was introduced in Eq. (2.2). The term with $d_1(d_2)$ corresponds to the first (second) grating constituting the Moiré grating; the amplitude of the refractive index profiles of each of these gratings is δn. Further,

$$\Delta n(z)=2\,\delta n\,\cos\left(\frac{2\pi}{\Lambda}\right), \tag{2.5}$$

$$\frac{1}{D}=\frac{1}{2}\left(\frac{1}{d_1}+\frac{1}{d_2}\right), \tag{2.6}$$

and Λ was defined in Eq. (2.3).

Since the grating is linearly chirped, $d_{1,2}$ depend on position according to

$$\frac{1}{d_i}=\frac{1}{d_i^0}+\alpha z \quad \text{where} \quad i=1,2, \tag{2.7}$$

where d_i^0 is a reference period and the chirp parameter α is the rate of change of $1/d$ with position. Thus the rapidly varying periodic component of the refractive index (period D) is a linear function of position (linearly chirped); we associate it with the uniform electric field in the electronic WSL. In contrast, the slowly varying periodic component of the refractive index (Δn) has a constant period Λ; we associate this component with the Bragg reflection. Now according to Eq. (2.2), the width of the photonic band gap $\kappa\propto\Delta n$ and it is thus periodic with Λ as well; this is the optical equivalent of the periodic crystal potential (line 4 of Table I).

The width of the photonic band gap is given by Eq. (2.2) and, using Eqs. (2.4)–(2.7), for a Moiré grating we can draw its two edges as a function of position [14]; the result is shown in Fig. 2(b) by the long- and short-dashed lines. As in Fig. 2(a), the overall linear ramp represents the linear chirp, while the sinusoidal behavior is associated with the Moiré effect. The periodic crossing of the long- and short-dashed lines indicates that consecutive half periods of the Moiré grating are π out of phase, but are otherwise identical [cf. Eqs. (2.2) and (2.4)]. Just as for electrons (Fig. 1), this periodicity spawns sidebands, which gives rise to additional (Bragg) reflections. In direct analogy to the closed orbits for electrons shown in Fig. 1(b), this leads to the periodic orbits for photons shown in Fig. 2(b).

Thus the closed photonic orbits in Fig. 2(b) have the same physical origin of the closed electronic orbits shown in Fig. 1(b). The analogy between the electronic and the optical case can now be taken further to obtain the desired result: There should be a ladder of closed orbits, separated in space by the superperiod Λ (line 5 of Table I) and in frequency by the chirp per Moiré period,

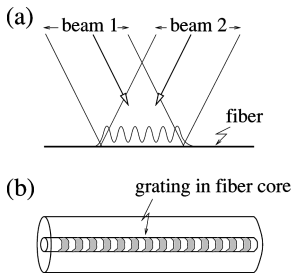

FIG. 3. (a) Schematic of the fabrication of a uniform optical fiber grating. The two beams lead to a sinusoidal interference pattern, which, by the photosensitivity of the core, leads to a grating. The periodic high- and low-intensity regions in the fiber core, which constitute the grating, are shown schematically in (b).

$$\Delta f=\frac{c}{2\overline{n}}\alpha\Lambda. \tag{2.8}$$

Thus our proposed structure shares the defining characteristics of the electronic WSL (discussed in the first paragraph) and we thus refer to it as an ''optical WSL.'' Three orbits of the type discussed above are indicated schematically by the solid lines in Fig. 2(b); as required, they are displaced by a Moiré period.

Now recall that adjacent half periods of a Moiré grating are out of phase, but are otherwise identical. We therefore expect two interleaved WSLs, one associated with the odd half periods [solid orbits in Fig. 2(c), say], and the other with the even ones [dash-dotted orbits in Fig. 2(c)]. The two WSLs cannot be distinguished. In effect, therefore, we observe an optical WSL in which the orbits are displaced by half a Moiré period; spectrally we expect to observe a ladder with rung spacing half of that in Eq. (2.8), corresponding to a spacing in wavelength of

$$\Delta\lambda_{\mathrm{WSL}}=\frac{\alpha\Lambda\lambda_B^2}{4\overline{n}}, \tag{2.9}$$

corresponding the chirp over half a Moiré period.

Recall that each WSL rung corresponds to a resonance between two ''mirrors,'' as in a Fabry-Pérot cavity. In measuring the transmission spectrum of a chirped Moiré grating therefore, we expect periodic high-transmission fringes spaced by $\Delta\lambda_{\mathrm{WSL}}$ [Eq. (2.9)], each associated with a WSL rung.

III. EXPERIMENTAL RESULTS AND ANALYSIS

The fabrication of fiber gratings relies on the photosensitivity of germanosilicate glass, such as that in the core of an optical fiber [21]. This process, which is not well understood, causes the refractive index to increase permanently under illumination by ultraviolet light at wavelengths around 193 nm and 244 nm. As illustrated in Fig. 3(a), by interfering two external beams, tuned around either of these wavelengths, at the fiber core, a sinusoidal intensity profile results. Because

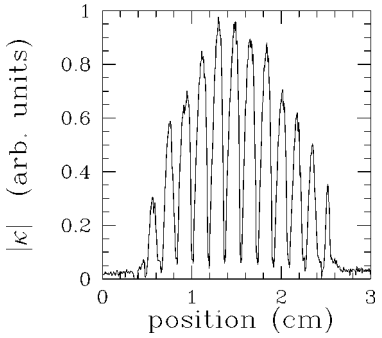

FIG. 4. Result of a side probe measurement of our Moiré grating, showing the magnitude of the refractive index modulation amplitude $\Delta n \propto |\kappa|$ [see Eq. (2.2)], as a function of position, with a resolution of 50 μm. The features in the figure result from the Moiré effect. The individual grating periods have a pitch of less than 1 μm.

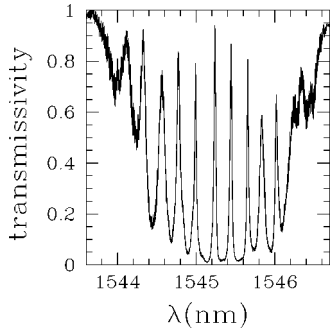

FIG. 5. Experimentally measured transmission spectrum of our chirped Moiré grating. The transmission peaks correspond to WSL rungs.

of the core's photosensitivity, a sinusoidal intensity profile leads to a periodic refractive index distribution, i.e., a grating [21]. A schematic of such a grating is shown in Fig. 3(b).

Recall that a Moiré grating is obtained when two gratings with slightly different periods are written in the same piece of fiber. We wrote each using two interfering beams of intense 244-nm light from a frequency-doubled Ar^+ laser [21]. Each grating was exposed by scanning the writing beam parallel to the fiber [22]. The grating length was limited to 22 mm by the optical components. Chirping was achieved by slowly changing the period of the interference pattern as the writing beam was translated.

From the transmission spectrum taken after writing a single chirped grating we inferred that $\delta n = 1.325 \times 10^{-4}$ [Eq. (2.4)], while the chirp was 0.105 nm/mm, corresponding to $\alpha \approx 1.3 \times 10^5$ m^{-2}. The uncertainty in these results is about 10%. This value for α implies that the grating period varies only by about 75 pm over the 22 mm length of the grating. Note that this is only a tiny fraction of the average grating period of about 500 nm [Eq. (2.1)]. It should also be noted that our writing method causes a decrease of the refractive index contrast at the edges of the grating. For this reason, δn, and thus κ [Eq. (2.2)], was modeled to have a parabolic shape vanishing at the grating's edges; we return to this below. The value for δn given above is the maximum magnitude of the refractive index modulation amplitude.

After analyzing the first chirped grating, we wrote the second chirped grating in the same piece of fiber to obtain a Moiré grating; the second grating was given a slightly different period by increasing the set tension of the fiber. The resulting Moiré grating was first investigated using a side probe technique, which lets one measure the magnitude of the refractive index modulation amplitude $|\Delta n|$, or, equivalently, $|\kappa|$ [Eq. (2.2)], as a function of position [23]. Figure 4 shows the result of this measurement. In Fig. 4, $|\kappa|$ is given in arbitrary units, as absolute measurements are quite difficult using this technique. The main features in Fig. 4 are due to the Moiré effect and are associated with the slowly varying function $\Delta n \propto \kappa$ [see Eqs. (2.2) and (2.5)]. Figure 4 shows that our Moiré grating is of good quality as the minima, corresponding to zero crossing of κ, are close to the noise floor. The Moiré grating is seen to have a period $\Lambda = 3.55 \pm 0.1$ mm and is roughly constant over the length of the grating. Figure 4 also confirms the nonuniform envelope of $|\kappa|$; recall that we approximate this envelope by a parabola that vanishes at the edges of the grating.

Shown in Fig. 5 is the measured transmission spectrum of our chirped Moiré grating. It exhibits nine clear transmission peaks, which are spaced by 0.212 ± 0.024 nm. The small standard deviation implies that the peaks are approximately equally spaced. To prove that these are the rungs of an optical WSL, we must show that the spacing equals the chirp over half a Moiré period. Given the chirp corresponding to $\alpha \approx 1.3 \times 10^5$ m^{-2}, as taken from the spectrum of the first grating, and the measured value $\Lambda = 3.55$ mm from the side scan (Fig. 4), using Eq. (2.9) we arrive at a fringe spacing $\Lambda_{\mathrm{WSL}} = 0.186$ nm, or 12% smaller than the measured value. This discrepancy can easily be accounted for by imperfect matching to the spectrum of the first of the two gratings comprising the Moiré grating and by imperfections in the writing of the second of these gratings, which we could not analyze in isolation.

We thus conclude that the transmission fringes in Fig. 5 are the rungs of an optical WSL, confirming the existence and the observation of an optical WSL. As an aside, we note that the spectrum of the first chirped grating alone does not exhibit the sharp, high-visibility features of Fig. 5. These features thus only occur when both gratings are present, consistent with our conclusion that the fringes in Fig. 5 are the rungs of an optical WSL.

Light propagation through Bragg gratings can be modeled using coupled-mode theory [24,15]. It allows one to work with slowly varying field amplitudes rather than with the electric field itself. Denoting the amplitudes of the forward and backward propagating modes by $\mathcal{E}_+$ and $\mathcal{E}_-$, respectively, it is found that these satisfy [15]

$$+ i \frac{d\mathcal{E}_+}{dz} + \delta(z)\mathcal{E}_+ + \kappa(z)\mathcal{E}_- = 0,$$

$$- i \frac{d\mathcal{E}_-}{dz} + \delta(z)\mathcal{E}_- + \kappa(z)\mathcal{E}_+ = 0, \qquad (3.1)$$

where the detuning $\delta(z)$ indicates the position of the local Bragg frequency with respect to a reference frequency. For a linearly chirped Moiré grating, κ follows from Eqs. (2.2) and (2.5) and varies sinusoidally with period Λ, indicating the Moiré effect, while δ is a linear function of position with a slope proportional to the chirp [14,15]:

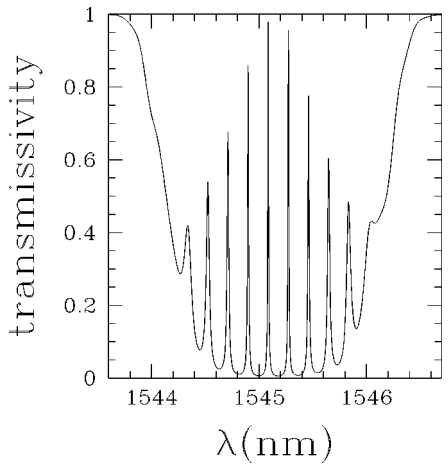

FIG. 6. Calculated transmission spectrum of a chirped Moiré grating with length 22 mm, a chirp of 0.105 nm/mm, a parabolic profile for κ that vanishes at the edges, and a maximum refractive index modulation $\delta n = 1.325 \times 10^{-4}$. The periods d_1, d_2 are determined from $\Lambda = 3.55$ mm and from the position of the spectrum via Eqs. (2.3) and (2.6).

$$\delta(z) = -2\pi\alpha z. \tag{3.2}$$

Figure 6 shows the calculated transmission spectrum, obtained from Eqs. (3.1). Recall that the parameters required for this calculation were determined from the side-probe measurement (Fig. 4) and from the spectrum of the single chirped grating, without any fitting parameters, and without using Fig. 5. The similarity between Figs. 5 and 6 confirms the inferred values of the key grating parameters.

Using coupled-mode theory, we have also studied the electric field associated with the WSL. We find that at each rung the field is strongly peaked, thus exhibiting the required localization (see Fig. 2). More importantly, the fields associated with adjacent fringes are displaced by half a Moiré period, thus further confirming the identification as the rungs of an optical WSL. The fields associated with the central WSL rungs are narrower than a Moiré period. Though for these resonances Wannier's semiclassical picture is thus not quite appropriate, they do exhibit the optical equivalent of electric field-induced localization [6]. While for the outer rungs the resonances are wider, the semiclassical regime, in which the resonances extend over many Moiré periods, requires a longer grating than that available for this experiment.

IV. DISCUSSION AND CONCLUSION

The description of the electronic WSL in Sec. I relies on the wave properties of the electron. Therefore, in principle, any type of wave can be used to observe the WSL. It is true that an equivalent description of the electronic WSL makes use of the transfer of electrons between bound states of quantum wells [8,10]. Such a description could also be applied to the optical WSL described here. The theory that would allow one to do so is currently a topic of active research [14,15,25,26]. Finally, note that one could provide a fully quantum electrodynamical description of the optical WSL, but such a description would not differ in an essential way from what was presented here, since in the classical limit bosons reduce to waves.

We have thus observed an optical WSL in a chirped Moiré grating. We have summarized comparisons between electronic and corresponding optical concepts in Table I. The optical WSL's crucial feature is the use of neutral species, thus avoiding the excitonic effects inherent in electronic WSLs. We can make the identification as an optical WSL because our structure exhibits the defining characteristics of the electronic WSL: The localized orbits are displaced by (half) a period, leading to spectrum with features occurring at (half) the chirp per Moiré period. The anomalous factor 1/2 is a feature unique to Moiré gratings and disappears in more general grating superstructures.

ACKNOWLEDGMENTS

We thank Simon Poole for making available to us the resources of Indx Propriety Ltd., John Sipe for many discussions regarding Wannier-Stark ladders, David Psaila for help with the final grating design, and Zourab Brodzeli for assisting with the side probe measurement.

[1] G. H. Wannier, *Elements of Solid State Theory* (Cambridge University Press, London, 1959), pp. 190–193.
[2] J. Callaway, *Quantum Theory of the Solid State* (Academic, New York, 1974), Chap. 6.
[3] See, e.g., C. F. Hart and D. Emin, Phys. Rev. B **37**, 6100 (1988).
[4] J. Zak, Phys. Rev. B **43**, 4519 (1991).
[5] J. M. Combes and P. D. Hislop, J. Phys. A **23**, 1501 (1990).
[6] E. E. Mendez, F. Agulló-Rueda, and J. M. Hong, Phys. Rev. Lett. **60**, 2426 (1988).
[7] M. M. Dignam and J. E. Sipe, Phys. Rev. Lett. **64**, 1797 (1990).
[8] Q. Niu, X.-G. Zhao, G. A. Georgakis, and M. G. Raizen, Phys. Rev. Lett. **76**, 4504 (1996).
[9] M. B. Dahan, E. Peik, J. Reichel, Y. Castin, and C. Salomon, Phys. Rev. Lett. **76**, 4508 (1996).
[10] M. Raizen, C. Salomon, and Q. Niu, Phys. Today **50** (7), 30 (1997).
[11] G. Monsivais, M. del Castillo-Mussot, and F. Claro, Phys. Rev. Lett. **64**, 1433 (1990).
[12] C. M. de Sterke, J. E. Sipe, and L. A. Weller-Brophy, Opt. Lett. **16**, 1141 (1991).
[13] See, e.g., G. E. Town, K. Sugden, J. A. R. Williams, I. Bennion, and S. B. Poole, IEEE Photonics Technol. Lett. **7**, 78 (1995).
[14] L. Poladian, Phys. Rev. E **48**, 4758 (1993).
[15] J. E. Sipe, L. Poladian, and C. M. de Sterke, J. Opt. Soc. Am. A **11**, 1307 (1994).
[16] E. Yablonovitch, Phys. Rev. Lett. **58**, 2059 (1987).
[17] F. Ouellette, Opt. Lett. **12**, 847 (1987).

[18] V. Jayaraman, Z.-M. V. Chuang, and L. A. Coldren, IEEE J. Quantum Electron. **29**, 1824 (1992).
[19] B. J. Eggleton, P. A. Krug, L. Poladian, and F. Ouellette, Electron. Lett. **30**, 1620 (1994).
[20] P. St. J. Russell, Phys. Rev. Lett. **56**, 596 (1986).
[21] See, e.g., R. J. Campbell and R. Kashyap, Int. J. Optoelectron. **9**, 33 (1994).
[22] J. Martin and F. Ouellette, Electron. Lett. **30**, 811 (1994).
[23] P. A. Krug, R. Stolte, and R. Ulrich, Opt. Lett. **20**, 1767 (1995).
[24] D. Marcuse, *Theory of Dielectric Optical Waveguides*, 2nd ed. (Academic, Boston, 1991).
[25] N. G. R. Broderick and C. M. de Sterke, Phys. Rev. E **55**, 3634 (1997).
[26] C. M. de Sterke, Phys. Rev. E (to be published).